Proceedings of COBEM 2011

21st International Congress of Mechanical Engineering
October 24-28, 2011, Natal, RN, Brazil

NUMERICAL SIMULATION OF THE INFLUENCE OF THE BLOOD FLOW PATTERN IN VENOUS VESSELS IN THE THROMBUS FORMATION

Thabata Coaglio Lucas, thabataclucas@yahoo.com.br
Daniel Leite Oliveira, ddd3_daniel@yahoo.com.br
Universidade Federal de Minas Gerais; Av. Antônio Carlos, 6627-31270-901 Belo Horizonte – MG. Brazil

Rudolf Huebner, rudolf@ufmg.br
Universidade Federal de Minas Gerais; Av. Antônio Carlos, 6627-31270-901 Belo Horizonte – MG. Brazil

Abstract. *A numerical investigation of Newtonian and non-Newtonian steady blood flow in a complete idealized three-dimensional venous model have recently been shown to provide prognostically relevant for hemodynamic data. The geometry reconstruction is essencial for the assessment of clinically relevant hemodynamic parameters. The blood flow patterns influence the development of thrombus that remains a significant problem in current clinical practice.This study is presented in in order to simulate numerically the influence of the blood flow pattern in venous vessels in the thrombus formation. Are acquired images of veins in Visible Human Project® to construct the geometry in in the software Solid Works®. The effects for two different sets of physiological parameters of laminar and turbulent blood flow was obtained running a computational fluid dynamics (CFD).Laminar Newtonian and non-Newtonian steady flow was adopted and compared with a turbulence flow model. The results show that shear stress gradient in non-Newtonian turbulence model, presented lower than non-Newtonian laminar flow.The shear stress distribution asymmetry,low shear stress, oscillatory shear strain rate and a combination of low velocity may also indicate areas at risk for thrombosis due to endothelial reorganization and venous stasis. These hemodynamics factors may contribute to further development of thrombus formation in venous vessels.*

Key words*: Computational flow simulation; venous flow; thrombus.*

1.INTRODUCTION

Traditionally, the internal jugular vein (IJV) has served as an indicator of right side cardiac function via measurement of central venous pressure and changes in the velocity of jugular venous flow. Recent studies have focused on either the position of the IJV to facilitate cannulation with a central venous catheter, or thrombosis of the IJV (Shreiber *et al.,* 2003*;* Lonyai *et al.*, 2010; Sharma *et al.*, 2010). Central venous catheter insertion is reported to be the most common cause of IJV or subclavian vein thrombosis. Venous thrombosis results from a disturbance of normal blood flow with subsequent activation of coagulation mechanism. Activated clotting factors collect in areas of sluggish or turbulent blood flow, thereby precipitating platelet aggregation.

These problems can be predicted, since numerical simulation provides an alternative way to obtain detailed flow patterns in hemodynamic conditions and may enable improved prediction of thrombosis and the ability to develop strategies to avoid these complications.

Another important aspect, in simulating blood flow in veins and in assessing its impact on shear stress, is to incorporate the nature of blood as a fluid. A correct description of blood rheology is the key to assess derived parameters as shear stress accurately which is one of the known platelet activing mechanisms that leads to thrombus formation (Fischer *et al.*, 2007; kagadis *et al.*, 2008; Bodnár *et al.*, 2010). There is a little information in the literature on the change in shear stress in venous vessels since shear stress may also indicate areas at risk for thrombosis due to endothelial reorganization and venous stasis. Generally, the non-Newtonian rheology becomes more pronounced when the shear rate is low and the geometry is small, complex and tortuous (Li *et al.*, 2007; Lin *et al.*, 2009).

According to non-Newtonian behavior, viscosity depends on the velocity gradient and varies along of the vessel (Vimmir and Jonásová, 2010). Henceforth, the variation depends on the applied flow conditions of the vein, the vascular geometry, and the flow particularities. However little research has focused the behavior of non-Newtonian flow venous in regions of high potential risk, as the internal jugular and superior vena cava veins, since they are specific regions of insertion of invasive devices in procedures as hemodialysis. Further adequate blood viscosity models are needed to capture the main flow characteristics at low strain rates, especially in the vein where the blood flow velocity is lower than in the arteries.

A variety of hemodynamic factors have been proposed in the development of thrombus formation, which includes recirculation zones, turbulence, low and oscillating shear stress and variations of the shear stress (Woo and Kyehan,2007; Lonyai *et al.*, 2010). However, the specific mechanisms whereby blood flow patterns influence the development of thrombus remain a major unsolved question in bioengineering.

While there are many factors that may affect risk for thrombosis, in this work we focus on hemodynamic factors, specifically changes in velocity, pressure, and shear stress in the veins, and locate and quantify regions of stasis to identify where potential risk for thrombosis occurs. We believe the identification of these regions is critical to predicting and preventing areas of thrombosis and occlusion in a patient specific manner. The aim of this study was to simulate numerically the influence of the blood flow pattern in venous vessels in the thrombus formation.

2.METHOD AND MATERIAL

2.1. Generation of three-dimensional model

Are acquired images of veins in Visible Human Project®, National Library of Medicine, licensed by bioengineering laboratory at Federal University of Minas Gerais (UFMG/BRAZIL). The program is the creation of complete, anatomically detailed, three-dimensional representations of the normal male and female human bodies.

Acquisition of transverse computerized tomography, magnetic resonance and cryosection images of representative male and female cadavers has been completed. The male was sectioned at one millimeter intervals, the female at one-third of millimeter intervals. In this work the internal jugular and superior vena cava were from the male model. The axial anatomical images are 2048 pixels by 1216 pixels where each pixel is defined by 24 bits of color, each image consisting of about 7.5 megabytes of data. The anatomical cross-sections are also at 1 mm intervals and coincide with the computerized tomography axial images. Were needed 250 cross-sections images to construct the three-dimensional model.

To create the three-dimensional geometry, the images were imported into the SolidWorks®software. The images were bounded by interpolation polynomial curves and overlapping in parallel planes. The spacing between these represented the physical distances between the images of cross-sections. Figure 1 illustrates the cross-section image from Visible Human Project® and the polynomial curves in blue outlining the internal jugular veins.

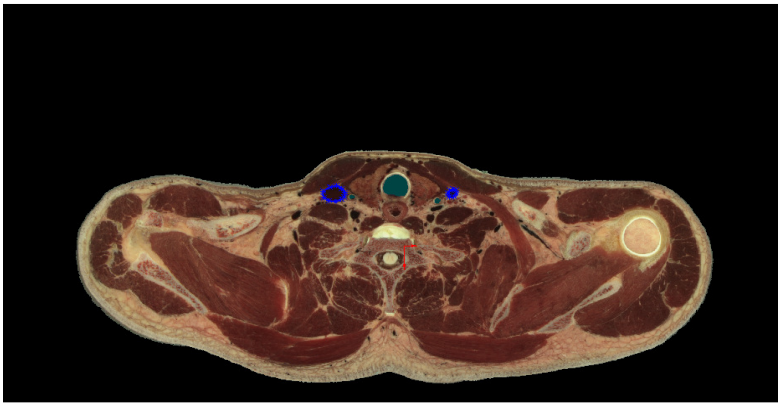

Figure 1: Cross-section image from Visible Human Project®

To construct the 3D model were required several features of Solid Works® that involves the union of the representative curves of the geometry that will generate the geometric solids. Figure 2 shows the three-dimensional geometric solid model of the right and left internal jugular vein, right and left subclavian vein and superior vena cava.

Figure 2: Three-dimensional geometric solid model of the right and left internal jugular vein, right and left subclavian vein and superior vena cava

2.2 Meshing and elements

Mesh independency study was carried out performing a number of simulations with different mesh size, starting from a coarse mesh and refining it until results were no more dependent on the mesh size. The computational mesh was constituted of tetrahedral elements and of prism elements have been introduced in the vicinity of walls to define flow parameters at veins walls more precisely. The mesh independence study was carried out by doubling the elements for the fluid domain and comparing the pressure distributions, shear stress, Y plus (for turbulence model) and velocity profiles along the wall. The results showed maximum 5% difference and in some parts of the flow field, the results agreed to <1%. The original mesh was used since tests have not yielded any significant differences that could affect the results of the computations conducted.

A boundary layer consisting of eight rows, with an expansion factor of 1.15(ratio between two consecutive layers near the wall) and a total depth of 2 mm, was generated. The total number of nodes exceeded 3,000,000. The number of the tetrahedrons elements was about 12,978,147 and the total of number of prisms were 10,638, 615. Figure 3(a) illustrates a volumetric mesh of the model and 3(b) a sample mesh of different densities in vein section and the prism element introduced in the vicinity of walls.

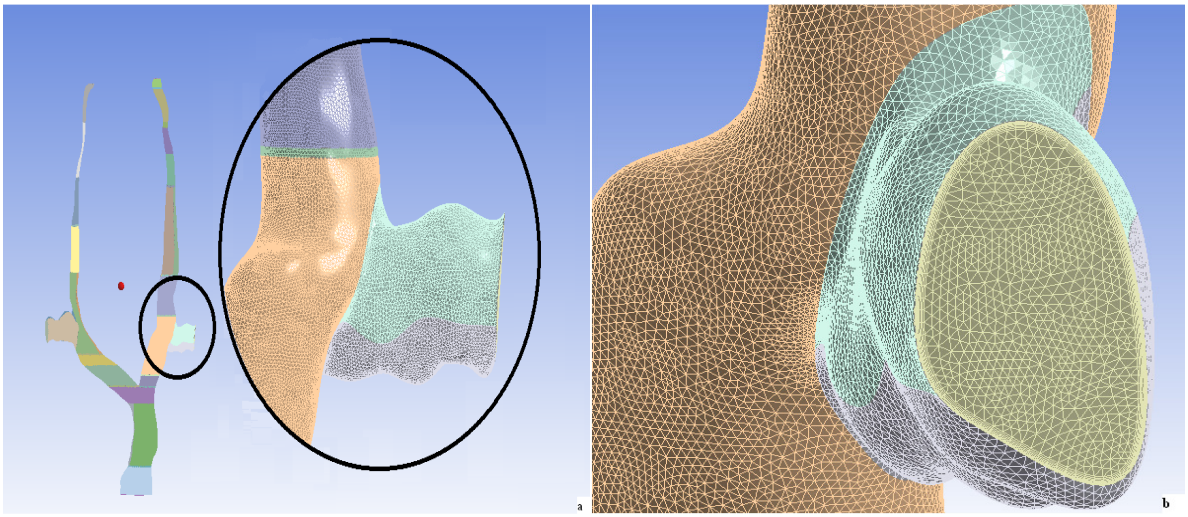

Figure 3: Mesh of the model (a) and the prism element introduced in the vicinity of walls (b)

2.3 Boundary conditions and flow models

The numerical solution of steady Navier-Stokes equations for momentum and mass conservation governing fluid motion under defined boundary conditions were solved by a control volume finite element (FVE) implemented in ANSYS® CFX 12 (ANSYS-Fluent Inc.,Lebanon,NH,USA).

Were conducted the flow field in the veins in four models of CFD simulation. Firstly the flow was assumed as laminar, steady and Newtonian with density of 1050kgm^{-3} and dynamic viscosity was of η = 0.00345Pas compared to the non-Newtonian flow, where the fluid's molecular viscosity $\eta(\dot{\gamma})$ is considered to be shear-dependent and given by the Correau-Yassuda model (Vimmir and Jonásová, 2010).

The Navier-Stokes equation of incompressible flows of a Newtonian fluid satisfies a linear relation between the shear stress and the deformation rate. The conservation of mass in Eq.(1) and momentum in Eq.(2) can then be expressed as:

$$\nabla.\vec{u} = 0 \tag{1}$$

$$\rho\vec{u}.\nabla\vec{u} = -\nabla p + \nabla.\left[(\mu + \mu_T)(\nabla\vec{u} + \nabla\vec{u}^T)\right] \tag{2}$$

Using the same parameters of laminar and steady flow was adopted the Carreau-Yassuda model to calculate the non-Newtonian viscosity. The C-Y model is more appropriate to simulate with better accuracy the shear rate and for to predict the viscosity (Wang and Bernsdorf, 2009; Valencia and Baeza, 2009).

This model is written as shown in the Eq. (3).

$$\frac{\mu-\mu_\infty}{\mu_0-\mu_\infty} = (1 + (\lambda\dot{\gamma})^a)^{(n-1)/a} \tag{3}$$

Where μ_0 and μ_∞ are the dynamic viscosities at zero and infinite shear rate respectively, $\dot{\gamma}$ is the shear rate and λ is a characteristic viscoelastic time of the fluid. At the critical shear rate 1/ λ the viscosity begins to decrease. The power law index parameters *a* and *n* can be determined from experimental data. In our simulations we apply the following set of parameters for blood analog fluid: μ_0=56 x10^{-3}Pas, μ_∞=3.45 x 10^{-3} Pas, a=1.25, n=0.22, λ=1.1902s (Wang and Bernsdorf, 2009; Valencia and Baeza, 2009).

In order to evaluate the scalar shear rate $(\dot{\gamma})$ was using in Eq.(4) the definition:

$$\dot{\gamma} = 2\sqrt{D_{II}} \tag{4}$$

Where D_{II} denotes the second invariant of rate of deformation tensor D = (1/2)(∇υ + (∇υ)^{T}). The second invariant D_{II} can be expressed for the incompressible flow,i.e., *tr*D =0,as Eq. (5)

$$D_{II} = \frac{1trD^2}{2} = \frac{1}{2}\, d_{ij}d_{ij}, \tag{5}$$

Where d_{ij} are the components of rate of deformation tensor *D* given by Eq. (6)

$$d_{ij} = \frac{1}{2}\left(\frac{\partial v_i}{\partial_{yj}} + \frac{\partial v_i}{\partial_{yi}}\right), i,j = 1,2,3. \tag{6}$$

The same parameters were applied in a turbulence flow model, *k-ω Shear Stress transport (SST)* in a Newtonian and non-Newtonian blood flow. *k* is the turbulent kinetic energy and *ω* the specific dissipation rate. This model accounts for the transport of the turbulent shear stress and gives highly accurate predictions of the onset and the amount of flow separation under adverse pressure gradients (Tan *et al.*, 2009). The shear stress transport model was adopted here, which is a superset of the standard *k-ω* model, and is more accurate and robust in overcoming near-wall treatment errors. This model accounts for the transport of the turbulent shear stress by the inclusion of transport effects into the formulation of the eddy viscosity.

Transport equations, one for the turbulent kinetic energy, *k*, Eq. (7), and specific dissipation rate *ω, Eq*. (8), including the model constants were based on Kagadis et al. (2008):

$$\frac{\partial(\rho k)}{\partial t} + \nabla.(\rho\bar{u}k) = \nabla.\left[\left(\mu + \frac{1}{2}\frac{\rho k}{\omega}\right)\nabla k\right] + P_k - (0.09)\rho k\omega \tag{7}$$

$$\frac{\partial(\rho k)}{\partial t} + \nabla.(\rho\bar{u}k) = \nabla.\left[\left(\mu + \frac{1}{2}\frac{\rho k}{\omega}\right)\nabla k\right] + \frac{5}{9}\frac{\omega}{k}P_k - (0.075)\rho\omega^2 \tag{8}$$

These equations represent the mean flow quantities only while modeling turbulence effects, without the need for the resolution of the turbulent fluctuations. In the 'eddy viscosity' description, turbulence consists of small eddies which are continuously forming and dissipating, the Reynolds stresses within these eddies are assumed to be proportional to mean velocity gradients. Equation of eddy viscosity model, such as *k-ω SST* is commonly used for the description of turbulence, as they offer a good compromise between numerical effort and computational accuracy.

The turbulent frequency is representing by Eq.9:

$$\mu_{turb=\frac{\rho k}{\omega}} \tag{9}$$

Where ρ is the turbulent viscosity, k is the turbulence kinetic energy and ω is the turbulence eddy frequency.

Regarding the boundary conditions, a steady laminar flow was simulated presuming rigid motionless walls. Recent studies concluded that when incorporating the wall motion, the overall characteristics of the shear stress distribution do not seem to change significantly (Tan *et al.*, 2009; Valencia and Baeza, 2009). Further the effect of pulsatility was also found to be small and to have a limited effect on local shear stress (Tan *et al.*, 2009; Valencia and Baeza, 2009). However the present study may still have overestimated the values of the wall shear stress, thus future work could include fluid structure interaction study in association with the transition model.

A no-slip condition was assumed at the wall. The pressure of 533.33Pa value was imposed at the outlet (physiological pressure of the superior vena cava). The velocity profile was assumed at the inlet. According to these

measurements, the mean inlet velocity is equal to the 0.1 m/s (inlet of the internal jugular end subclavian veins). The convergence was considered achieved when the conservation equations of mass and momentum and the turbulence eddy frequency and turbulence kinetic energy were satisfied, which was considered to have occurred when the normalized residuals were set as 10^{-4}.
Equations (10) and (11) shows the boundary conditions of turbulence model were:

$$k = \frac{3}{2}\left[I_{def}\max((U_s|U_{IG}.U_\omega)\right]^2 \tag{10}$$

Where I_{def} is a default, in ANSYS® CFX 12, of the turbulent intensity of 5%,U_s is a minimum clipping velocity of 0.01m/s to avoid a result of zero for the turbulent kinetic energy when an initial velocity value of zero exists, U_{IG} is the velocity initial guess and U_ω is the product of the simulation average length scale and the rotation rate. This term is designed to produce a suitable velocity scale for rotating domains.

$$\omega = \frac{k}{\nu(\mu_T/\mu)} \tag{11}$$

Where k is the turbulence kinetic energy, ν is the kinematic viscosity and μ_T/μ is the eddy viscosity ratio, which is set to 10 by default.

3. RESULTS AND DISCUSSIONS

Figure 4 shows the shear stress in Newtonian (a) and non- Newtonian laminar flow simulations (b) and in Newtonian (c) and non- Newtonian (d) turbulent flow simulations.

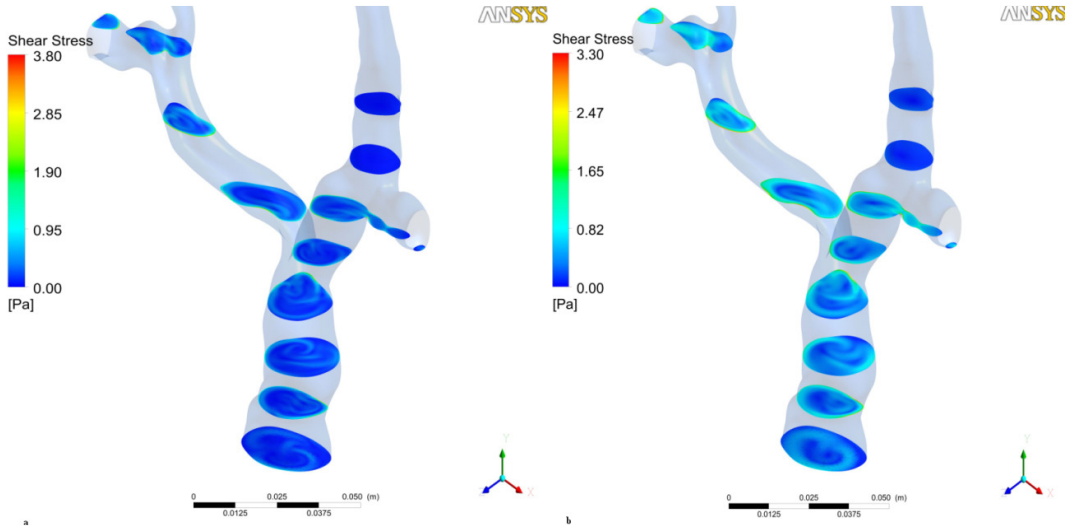

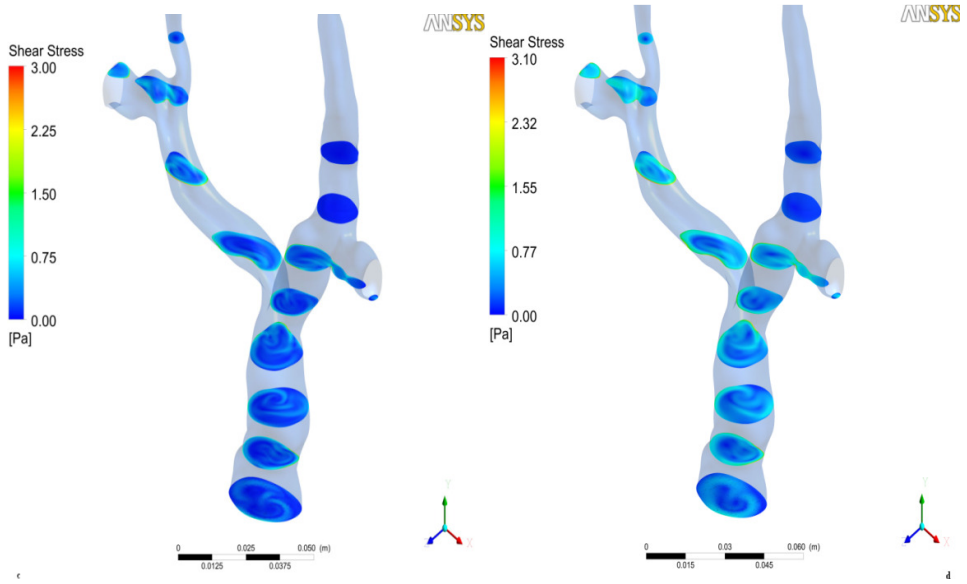

Figure 4: Comparison between shear stresses in Newtonian (a) and non- Newtonian laminar flow simulations (b) and in Newtonian (c) and non- Newtonian (d) turbulent flows

The shear stress distribution shows asymmetry and the maximum value was at upper region of the left internal jugular vein, where there is area reduction within the vein and it reaches 162. 140 Pa. The minimum value of the model was around 0.001Pa in the Newtonian laminar flows. These values are realistic from physiological point of view and therefore the results are representative for the flow in internal jugular veins.

As shown on the plans of the Fig. 4, most venous regions have low shear stress in all models. In the non-Newtonian flow the maximum value decreases 21% and the minimum value increased 50% compared Newtonian laminar flow. The shear stress gradient decreases in the non-Newtonian flow. It is important to comment that many data points to large variations of shear stress as being highly relevant indicators of risk sites for thrombus formation (Lonyai *et al.*, 2010; Politis *et al.*, 2007). Further the gradients of the shear stress give a measure of the spatial variations. A large local gradient means large local changes of shear forces, which is expected to be disadvantageous for the cell of the vessel wall.

The low shear stress regions may also indicate areas at risk for thrombosis due to endothelial reorganization and venous stasis. Studies have indicated that low shear stress induces aggregation of leukocytes on endothelium and a consequent up regulation of inflammatory markers like tissue factor that may increase risk for thrombosis.

In our study the SST model was adopted since provides better results near the surface wall which was of significant importance to assess the shear stress and shear strain rate in turbulence flow description. In comparison, shear stress gradient in non-Newtonian turbulence model, presented lower than non-Newtonian laminar flow (the maximum value (124.063 Pa) decreases 21% and the minimum value increased 34% (0.006Pa). In the turbulent Newtonian flow, the shear stress decreases 8% in the maximum value and increase 50% in the minimum value.

The turbulent flows can generate vortices sufficient strength to create a negative flux at the flow boundary (kagadis *et al.*, 2008). In the present study, the flow was leaving the domain at all points along the outflow boundary and the simulation was stable all the time.

Interestingly, clinical data, confirm areas we found to be at greatest risk for thrombosis when central venous catheters cannulation due to low gradient of shear stress and very low and very high shear stress values in certain regions of the vein. In the present study, a combination of low velocity (0 - 0.270m/s) and low shear stress was observed in all models. Values above 0.200 m/s were in turbulent flow. The difference of average velocity values between Newtonian and non-Newtonian flow were not significant.

The maximum values of shear strain rate were about $620s^{-1}$ and $510s^{-1}$ for laminar flows Newtonian and non-Newtonian respectively. For the turbulent flows the maximum shear strain rate was 480 s^{-1} and 458 s^{-1} in Newtonian and non-Newtonian flows respectively. It is well known that blood behaves as a non-Newtonian fluid, particularly at low shear rates, that is, less than 100 s^{-1} (Tam *et al.*, 2009; Bernsdorf and Wang, 2009;Vimmir and jonásová, 2010).Some models take blood flow to be Newtonian, on the assumption that the shear rates are greater than 100 s^{-1}. In the present study the most of the values in the non-Newtonian laminar and turbulent flows along the model as a whole were in average between 20-96 s^{-1} whereas in Newtonian models were in average between 134-620 s^{-1}. The oscillatory shear index may influence in the formation of fibrin clots on the surface of the device when inserted into the vein. This

fact could explain the high rate of thrombus formation in hemodialysis central venous catheters. However flow characteristics at shear strain rate have demonstrated the necessity of describing the blood rheology in a more accurate way.

Moreover is interesting to note that clots begins to form in blood flow with a shear strain rate from 0.1 s^{-1} to 20 s^{-1} which correspond to shear stresses ranging from 0.0012 Pa to 0.024 Pa (Xu *et al.*, 2009).Further for a flow rate of 0.05 m/s flow vorticity is observed to bring some platelets to the back side of the clot (Xu *et al.*, 2009). However, the flow vorticity is weak and flow does not flush larger blood cells to the back side of the clot. The effect of the low rate on the complexity of the clot structure is observed in the development of thrombi generated following vascular injury in experimental animals (Tam *et al.*, 2009; Xu *et al.*, 2009).

The overall pressure distributions differences between laminar and turbulent Newtonian flow were minimal. The values were about 7693.654 Pa -112.297Pa. However in the non-Newtonian laminar and turbulent flows the pressure gradient decreases (6182.619Pa - 150.286Pa). The cross-sections planes inserted within the domain showed an increase of pressure values over the plans in the non-Newtonian flow as shown in Fig (5).

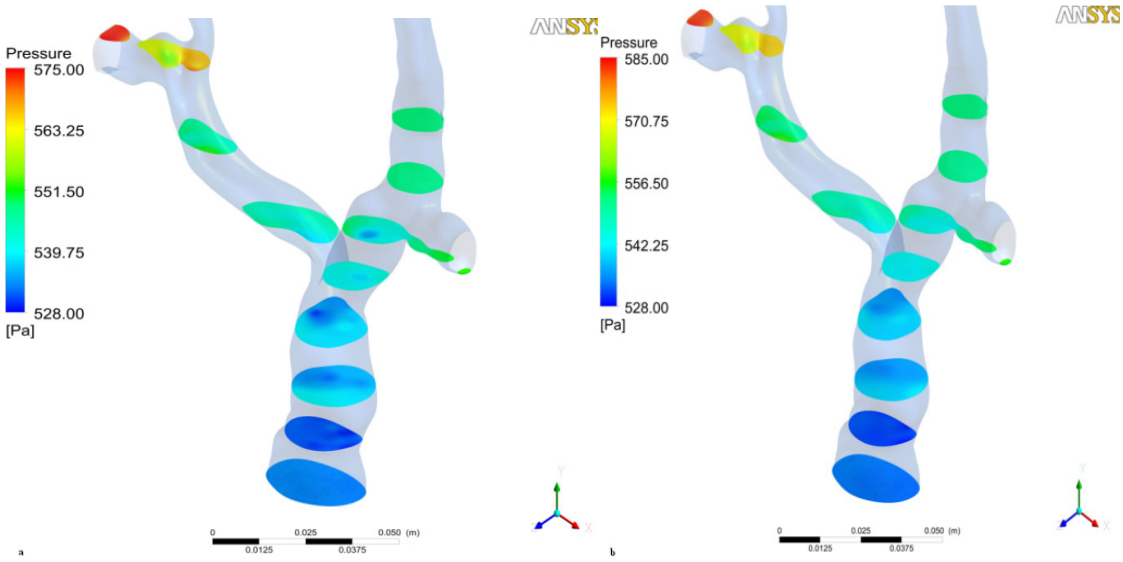

Figure 5: The cross-sections plane within the domain in the laminar newtonian flow (a) and laminar non-Newtonian flow.

The results of maximum blood pressure from this study agreed well with published clinical measurement,indicating that the model is physiologically realistic in internal jugular veins and superior vena cava.The ability to accurately predict the hemodynamic in such an environment is of interest to clinicians and researches alike.

4. LIMITATIONS

The presented results refer to select model of vein in on certain boundary conditions that which often depends on the physiological conditions and anatomy of each patient. The inlet blood flow velocity was assumed to be constant. Indisputably, the inlet flow velocity profile affects the flow analysis, particularly in regions close to the inlet. It is expected that the flow pattern will be altered with the vessel diameter and corresponds inlet blood flow velocity values of the systole and diastole of the cardiac cycle. Therefore, all transient physiological parameters have to be taking into account in future works for, i.e., wall compliance and pulsatile flow. Further the comparison of the hemodynamic parameters in geometries based on different imaging techniques is fully representative for analysis of the imaging technique impact for the assessment of venous flow.

Finally, different molecular viscosity models were not compared and only the Carreau-Yassuda model was adopted.

5. CONCLUSION

All numerical results presented in this paper confirmed the significance of inlet Reynolds numbers by analysis of Newtonian and non-Newtonian blood flow with corresponding average physiological parameters.

The conduct numerical investigation confirm a possibility of modeling the geometry and of obtaining results that enable an analysis of the effect of the flow conditions to better understand the thrombus formation in venous vessels.

In addition to improving our understanding of the thrombus formation in clinical arena, this model may help in the development of new strategies to avoid these complications. The computational model showed a market difference in the distribution of the shear stress, oscillatory shear strain rate, velocity and pressure in the veins which are hemodynamic factors predisposed for thrombus development. Result indicate that by using computational fluid dynamics, differing risk factors can be determined for patients with different anatomies and catheters positions when inserted in veins.

6. REFERENCES

Bernsdorf, J. and Wang, D., 2009. "Lattice Boltzmann simulation of steady non-newtonian blood flow in a 3D generic stenosis case". *Computers and Mathematics with Applications*, Vol. 58, pp. 1030-1034.

Bodnár, T. *et al*., 2010. "On the shear-thinning and viscoelastic effects of blood flow under various flow rates". *Applied Mathematics and Computation,* Vol. 217, No. 1, pp. 5055-5067.

Fischer, P.F. *et al*., 2007. "Simulation of high-Reynolds number vascular flows". *Computer Methods in Applied Mechanics and Engineering*, Vol. 196, No. 32, pp. 3049-3060.

Kagadis, C. G. *et al*., 2008. "Computational representation and hemodynamic characterization of in vivo acquired severe stenotic renal artery geometries using turbulence modeling". *Medical Engineering & Physics*, Vol. 30, pp. 647 - 660.

Li, M. X. *et al*., 2007. "Numerical analysis of pulsatile blood flow and vessel wall mechanics in different degrees of stenoses". *Journal of Biomechanics*, Vol. 40, No. 16, pp. 3715 - 3724.

Lin,S.K.,Chuang,Y.and Yang,F.,2009. "Hemodynamics of the Internal Jugular Vein: An Ultrasonographic Study*"*. *Tzu Chi Medical Journal*,Vol. 21, No.4, pp.317-322.

Lonyai,A. *et al*.,2010."New Insights into Pacemaker Lead-Induced Venous Occlusion: Simulation-Based Investigation of Alterations in Venous Biomechanics". *Cardiovascular Engineering*, Vol.10, No.2, pp.84-90.

Polits,A.K. *et al*.,2007."Numerical modeling of simulated blood flow in idealized composite arterial coronary grafts: Steady state simulations". *Journal of Biomechanics*, Vol.40, pp.1125-1136.

Sharma,K.S., *et al*., 2010. "Chronic brainstem ischemia in subclavian steal syndrome*"*. *Journal of Clinical Neuroscience*,Vol. 17, pp.1339-1341.

Shreiber,S.J. *et al*,2003. "Extrajugular pathways of human cerebral venous blood drainage assessed by duplex ultrasound*"*. Journal of Applied Physiology,Vol.94, pp.1805-1805.

Tan,F.P.P. *et al*.,2009. "Analysis of flow patterns in a patient-specific thoracic aortic aneurysm model*"*. *Computers and Structures*, Vol.87, pp.680-690.

Valencia, A. and Baeza,F.,2009."Numerical simulation of fluid-structure interaction in stenotic arteries considering two layer nonlinear anisotropic structural model". *International Communications in Heat and Mass Transfer*,Vol.36, No.2, pp.137-142.

Vimmir, J. and Jonásová, A., 2010."Non-newtonian effects of blood flow in complete coronary and femoral bypasses*"*.*Journal Mathematics and Computers in Simulation*, Vol.80, No. 3, pp.1324-1336.

Xu, Z. *et al*., 2009. "Study of blood flow impact on growth of thrombi using a multiscale model". *The Royal Society of Chemistry*,Vol. 5, pp. 769-779.

Woo, J. and Kyehan, R., 2007. "Numerical analysis of forced injection of enzyme during thrombolysis". *Computers in Biology and Medicine*,Vol.37, No.3, pp.655-662.

7. RESPONSABILITY NOTICE

The authors are the only responsible for the printed material included in this paper.